

## A LOW-TEMPERATURE SOL-MICROWAVE METHOD FOR ULTRA-SMALL RUTILE TITANIUM DIOXIDE NANOPARTICLES

<sup>1,2</sup>Aiswarya Vijayakumar THELAPPURATH, <sup>1</sup>Naděžda PIZÚROVÁ

<sup>1</sup>*Institute of Physics of Materials, v.v.i., Czech Academy of Sciences, Brno, Czech Republic, EU, [pizurova@ipm.cz](mailto:pizurova@ipm.cz)*

<sup>2</sup>*Central European Institute of Technology, Brno University of Technology (CEITEC), Brno, Czech Republic, EU*

<https://doi.org/10.37904/nanocon.2024.5001>

### Abstract

The rutile phase of TiO<sub>2</sub> can generally be obtained by high-temperature calcination of anatase nanoparticles. However, calcination undoubtedly leads to agglomeration and growth, hence increasing particle size. So, fabrication of rutile titania at low temperatures is of great importance since the formation of bigger particles can be avoided. Here, ultra-small rutile TiO<sub>2</sub> nanoparticles (NPs) of ~ 5 nm have been synthesized using a sol-microwave method at low temperature (150 °C). These rutile TiO<sub>2</sub> NPs have shown no surface defects, such as trivalent titanium (Ti<sup>3+</sup>) ions and oxygen vacancies. The resulting samples were analyzed by the following methods: X-ray diffraction (XRD) to determine the crystallinity and phase composition, Raman spectroscopy to refine the phase composition, X-ray Photoelectron Spectroscopy (XPS) to identify oxidation states and phase composition in surface layers, and High-Resolution Transmission Electron Microscopy (HRTEM) to study morphology, phase analysis, and surface quality assessment.

**Keywords:** TiO<sub>2</sub> nanoparticles, rutile, low temperature, microwave synthesis, defect free

### 1. INTRODUCTION

Nanoscale TiO<sub>2</sub> is a very well-known and well-researched material due to its unique physical, [1] chemical, [2] optical [3] and electrical properties,[4] and chemical and thermal stability, [5,6] which found application in various fields, including photocatalysis,[7] electrochemistry, [8,9] and production of cosmetics [10] pigments, [11] and biomedicine [12] Furthermore, titanium oxide nanoparticles also exhibit unique surface chemistry and morphologies [13]. The specific surface area and surface-to-volume ratio increase dramatically as the size of a material decreases [14]. The high surface area accomplished by small particle size is favorable to various applications [15]. Thus, the performance of TiO<sub>2</sub> in its applications is predominantly influenced by the sizes of the building units, apparently at the nanometer scale. TiO<sub>2</sub> exists in several polymorphs [16]. Due to the novel characteristics and promising properties, naturally occurring polymorphs such as rutile, anatase and brookite have been widely synthesized [17]. From a thermodynamic point of view, rutile is the more stable phase, whereas anatase and brookite are metastable at all temperatures and transform to rutile when heated [18]. Rutile phase is the only high refractive index phase of titania [19]. Moreover, it has higher relative permittivity and ultraviolet ray absorption rate [20,21]. Accordingly, it is important to obtain and investigate rutile TiO<sub>2</sub> nanoparticles. The widely known method for the preparation of nano-sized rutile TiO<sub>2</sub> is the phase transformation from anatase at higher temperatures [22]. This method leads to the formation of large particle size, agglomeration, and low surface area [23]. Therefore, the fabrication of rutile titania at low temperature is significant.

There are a few methods reported to synthesize rutile TiO<sub>2</sub> nanoparticles at low temperature including hydrothermal method, [24] sol-gel synthesis, [25] chemical precipitation route, [26] and low-temperature precipitation method [27]. We hereby report a facile and easily reproducible microwave-assisted synthesis of rutile TiO<sub>2</sub> NPs with a size less than 5 nm at low temperature. The microwave (MW) synthesis method

dramatically reduces reaction times, increases product yields, and enhances product purities compared to conventionally heated experiments [28]. In addition, the method is economical, rapid, less time-consuming, and atom-economical for preparing nanostructures [29]. Furthermore, this work investigates the structural characteristics and morphological properties of the synthesized ultra-fine rutile TiO<sub>2</sub> NPs.

## 2. EXPERIMENTAL

### 2.1 Materials

Titanium (IV) acetylacetonate (ca. 63% in Isopropyl alcohol, TCI), Isopropanol (99.5%, anhydrous, Merck), Ammonium hydroxide (NH<sub>4</sub>OH) (25%, Lach:ner), Ethanol (99.8%, Penta Chemicals) and DI water were used for the experiment. All the chemicals were used as received.

### 2.2 Synthesis of Titanium oxide nanoparticles

Titanium (IV) acetylacetonate was mixed with 100 mL of isopropanol, 14.4 mL of distilled water and 25 mL of NH<sub>4</sub>OH solution in a 250 mL beaker and stirred at 500 rpm for 5 minutes to create a homogenous reaction mixture. Then, the resulting sol was introduced in a 30 mL glass vial sealed with a snap cap comprising silicone septum. The filled vial was enclosed into a synthesis reactor, and the reactor was heated to the temperature of 150 °C, followed by microwave heating at the same temperature for 10 min at 900 rpm. The obtained product was dried in an oven at 100 °C for 2 hrs. After that, the dried sample was washed using DI water and ethanol to remove organic or inorganic impurities and dried for 2 h at 100 °C.

### 2.3 Characterization

The TiO<sub>2</sub> NPs have been synthesized in an Anton Paar Monowave-400 microwave reactor. All the NPs were analyzed using the X-ray diffractometry (XRD; Smart Lab 3 kW from Rigaku, Japan), which was set in Bragg-Brentano geometry with Cu-K $\alpha$  radiation ( $\lambda = 0.154$  nm) and fitted with the Dtex-Ultra 1D detector. The Cu radiation was powered by a 30-mA current and a 40-kV voltage. The diffraction patterns were acquired using a step size of 0.02° and a scanning speed of 4°/min from 20° to 80°. Phase analysis and chemical composition were performed using the PDF2 database. A Witec alpha-300R instrument (WITec, Ulm, Germany) was used for Raman spectroscopy. Raman spectra were recorded in continuous scanning mode at a laser excitation wavelength of 532 nm. A 100x objective lens focused the laser beam, producing a spot about 1  $\mu$ m in diameter. The measurement signal was reconstructed using 50 accumulations and a 20 s integration period. The chemical composition investigation was conducted using X-ray photoelectron spectroscopy (XPS, Kratos Analytical Axis Supra), and the spectra were calibrated against the C 1s peak (284.8 eV) using the CasaXPS software. Transmission electron microscopy (TEM) was used to confirm the NP size and size distribution and impart detailed structural characterization. TEM images were carried out on a TALOS F200i (ThermoFisher Scientific) instrument, operating at an acceleration voltage of 200 kV. The TEM samples were prepared by putting a drop of sample solution on a commercially prepared Cu grid coated with an amorphous carbon layer. The corresponding filtered Fast Fourier transform patterns were evaluated with JEMS software.

## 3. RESULTS AND DISCUSSION

To accomplish low-temperature synthesis for nano-sized rutile TiO<sub>2</sub>, a sol- microwave-assisted method of synthesis has been designed and executed at the temperature of 150 °C, using titanium (IV) acetylacetonate as the precursor and ammonium hydroxide as precipitating agent, followed by heating at 100 °C. The sample was yellow in colour.

### 3.1 X-ray diffraction

**Figure 1A** shows the XRD patterns of the synthesized TiO<sub>2</sub> samples. The broad diffraction peaks can be attributed to the particles' low crystallinity or relatively small size. **Figure 1A** revealed that the sample

possessed an intense peak at  $48.5^\circ$  corresponds to rutile [30] and another broad rutile peak at  $62^\circ$  [31]. The phase analysis conducted with an X-ray diffraction method confirmed a small crystallite size (less than 5 nm) in the entire sample. The significant peak broadening does not allow us to confirm the purity of the rutile phase. Hence, the Raman spectra were recorded to confirm the presence of any additional phase.

### 3.2 Raman spectroscopy

Raman spectroscopy was also carried out further to understand the phase of  $\text{TiO}_2$  (**Figure 1B**). The Raman spectra show broad peaks at around  $\sim 260 \text{ cm}^{-1}$  (second-order Raman scattering of rutile),  $\sim 450 \text{ cm}^{-1}$  ( $E_g$  rutile),  $\sim 620 \text{ nm}$  ( $A_{1g}$  rutile) [32,33] and a broad band in the  $600\text{-}750 \text{ cm}^{-1}$  originated from the silica substrate used for Raman analysis [34]. According to the previous report, the second-order Raman scattering peak of rutile is slightly shifted to a higher wavenumber, possibly because of the influence of the precipitating agent ammonium hydroxide.

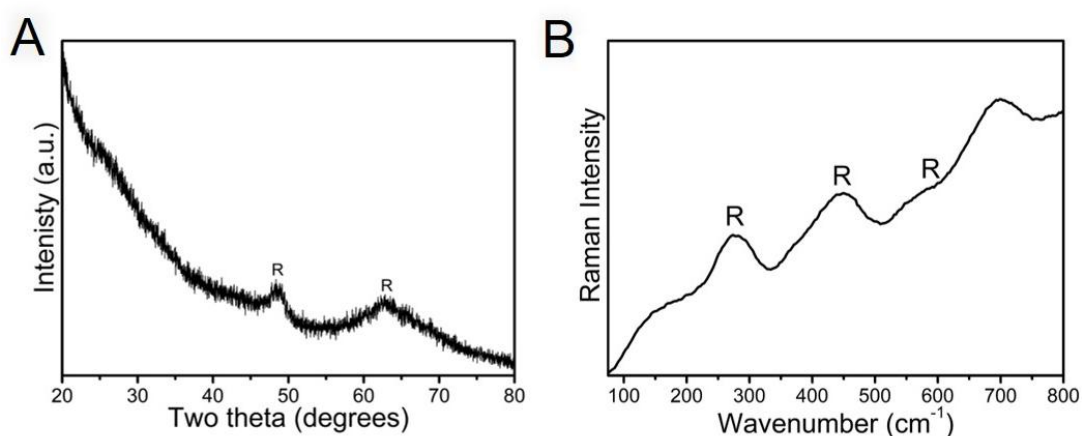


**Figure 1** A) X ray diffraction and B) Raman spectrum of rutile (R)  $\text{TiO}_2$

### 3.3 X-ray photoelectron spectroscopy

XPS spectra have been recorded for the synthesized rutile  $\text{TiO}_2$  NPs. **Figure 2** represents the wide,  $\text{Ti}2p$  and  $\text{O}1s$  XPS of the sample. The rutile  $\text{TiO}_2$  possessed  $\text{Ti}2p$  characteristic peaks corresponding to  $\text{Ti}^{4+}$ . The  $\text{Ti}2p_{3/2}$  and  $\text{Ti}2p_{1/2}$  were observed at  $458.78 \text{ eV}$  and  $464.53 \text{ eV}$  [35]. No indication of  $\text{Ti}^{3+}$  was seen. In  $\text{O}1s$ , peaks ascribed to  $\text{Ti-O-Ti}$ , and  $\text{Ti-OH}$  were found at  $530.24 \text{ eV}$ , and  $531.28 \text{ eV}$ , respectively [36].

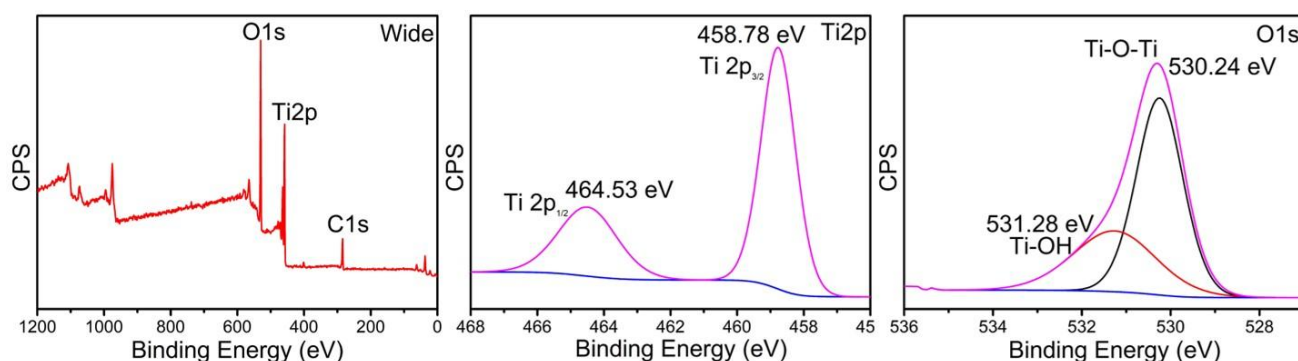


**Figure 2** Wide,  $\text{Ti}2p$  and  $\text{O}1s$  XPS of rutile  $\text{TiO}_2$

### 3.4 Transmission electron microscopy

Transmission electron microscopy measurements were used to confirm the morphology, size, and phase of the  $\text{TiO}_2$  nanoparticles. **Figure 3A** shows the clusters of ultrasmall nanoparticles, where heterogeneity in size

and shape can be observed. The obtained nanoparticles were nearly spherical morphology with an average diameter of 5 nm. **Figure 3B** is a high-resolution TEM (HRTEM) image of a single particle. Additionally, in **Figure 3C – 3E**, the Fast Fourier transform (FFT) over the crystalline areas was carried out to validate the presence of the TiO<sub>2</sub> rutile phase.

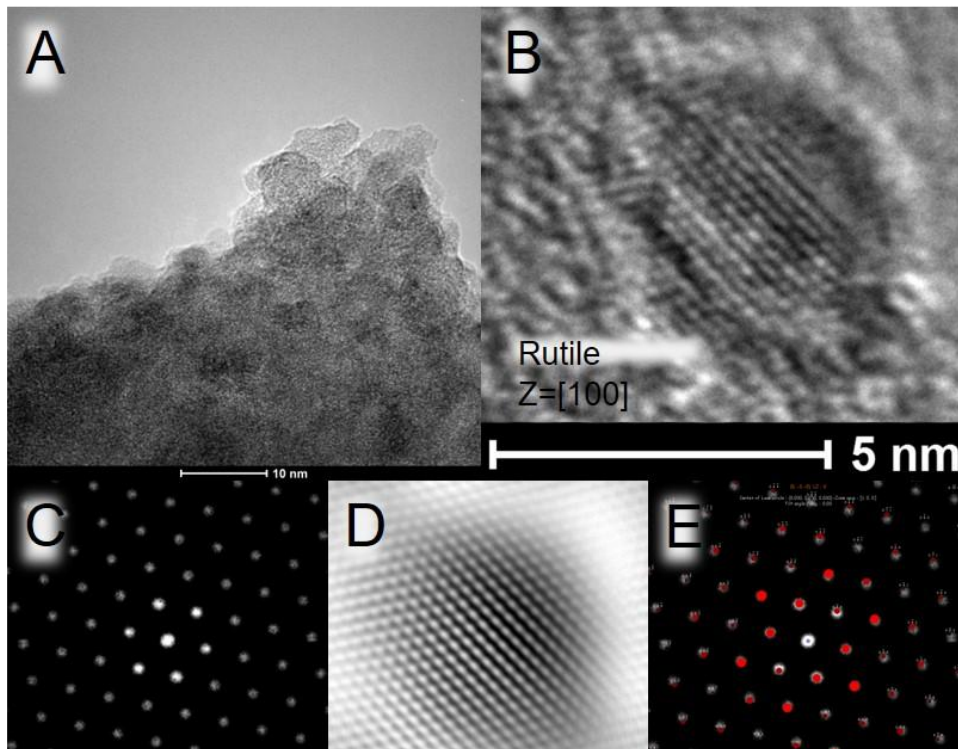


**Figure 3** A) TEM, B) HRTEM of selected nanoparticle, C) filtered FFT pattern, D) inverse filtered FFT pattern, and E) filtered FFT pattern evaluated as the rutile TiO<sub>2</sub> phase in the [100] crystallographic direction.

#### 4. CONCLUSIONS

A facile reproducible sol-microwave method has been developed to synthesize rutile TiO<sub>2</sub> NPs at low temperature. These rutile NPs were nearly spherical in shape with ~ 5 nm in size. Furthermore, these rutile TiO<sub>2</sub> NPs possessed only Ti<sup>4+</sup> and stoichiometric oxygen. In other words, these rutile NPs were observed free from defects such as trivalent titanium ions (Ti<sup>3+</sup>) and oxygen vacancies.

#### ACKNOWLEDGEMENTS

*The work was supported with the Czech Science Foundation, project No. 21-31852J and CzechNanoLab project LM2018110 funded by MEYS CR is gratefully acknowledged for the financial support of the measurements/sample fabrication at CEITEC Nano Research Infrastructure.*

#### REFERENCES

- [1] GUERIDI, B., BOUFERRACHE, K., GHEBOULI, M. A., ROUABAH, F., SLIMANI, Y., CHIHI, T., ... & BENALI, A. Physical properties of rutile-TiO<sub>2</sub> Nanoparticles and effect on PVA/SiO<sub>2</sub> Hybrid films synthesized by sol-gel method. *High Energy Density Physics*. 2024, 101122.
- [2] HSU, C. Y., MAHMOUD, Z. H., ABDULLAEV, S., ALI, F. K., NAEEM, Y. A., MIZHER, R. M., ... & HABIBZADEH, S. Nano titanium oxide (nano-TiO<sub>2</sub>): a review of synthesis methods, properties, and applications. *Case Studies in Chemical and Environmental Engineering*. 2024, 100626.

- [3] TRIPATHI, A. K., SINGH, M. K., MATHPAL, M. C., MISHRA, S. K., & AGARWAL, A. Study of structural transformation in TiO<sub>2</sub> nanoparticles and its optical properties. *Journal of Alloys and Compounds*. 2013, vol. 549, pp. 114-120.
- [4] REDDY, K. M., MANORAMA, S. V., & REDDY, A. R. Bandgap studies on anatase titanium dioxide nanoparticles. *Materials Chemistry and Physics*. 2003, vol. 78, no. 1, pp. 239-245.
- [5] THAKUR, N., THAKUR, N., KUMAR, A., THAKUR, V. K., KALIA, S., ARYA, V., ... & KYZAS, G. Z. A critical review on the recent trends of photocatalytic, antibacterial, antioxidant and nanohybrid applications of anatase and rutile TiO<sub>2</sub> nanoparticles. *Science of The Total Environment*. 2024, 169815.
- [6] FAROOQ, N., KALLEM, P., UR REHMAN, Z., KHAN, M. I., GUPTA, R. K., TAHSEEN, T., ... & SHANABLEH, A. Recent trends of titania (TiO<sub>2</sub>) based materials: A review on synthetic approaches and potential applications. *Journal of King Saud University-Science*. 2024, 103210.
- [7] TUNTITHAVORNWAT, S., SAISAWANG, C., RATVIJITVECH, T., WATTHANAPHANIT, A., HUNSOM, M., & KANNAN, A. M. Recent development of black TiO<sub>2</sub> nanoparticles for photocatalytic H<sub>2</sub> production: An extensive review. *International Journal of Hydrogen Energy*. 2024, vol. 55, pp. 1559-1593.
- [8] PUTJUSO, T., PUTJUSO, S., KARAPHUN, A., & SWATSITANG, E. Influence of Li concentration on structural, morphological and electrochemical properties of anatase-TiO<sub>2</sub> nanoparticles. *Scientific Reports*. 2024, vol. 14, no. 1, 11200.
- [9] ZHU, Y., LIU, T. H., ZHOU, W., SHI, M., WU, M., SHI, P., ... & LIN, C. T. An "On-Site Transformation" Strategy for Electrochemical Formation of TiO<sub>2</sub> Nanoparticles/Ti<sub>3</sub>C<sub>2</sub>T<sub>x</sub> MXene/Reduced Graphene Oxide Heterojunction Electrode Controllably toward Ultrasensitive Detection of Uric Acid. *Small Structures*. 2024, 2400034.
- [10] BERARDINELLI, A., & PARISI, F. TiO<sub>2</sub> in the food industry and cosmetics. In *Titanium Dioxide (TiO<sub>2</sub>) and Its Applications*. Elsevier. 2021, pp. 353-371.
- [11] GÁZQUEZ, M. J., BOLÍVAR, J. P., GARCIA-TENORIO, R., & VACA, F. A review of the production cycle of titanium dioxide pigment. *Materials Sciences and Applications*. 2014.
- [12] SAGADEVAN, S., IMTEYAZ, S., MURUGAN, B., ANITA LETT, J., SRIDEWI, N., WELDEGEBRIEAL, G. K., ... & OH, W. C. A comprehensive review on green synthesis of titanium dioxide nanoparticles and their diverse biomedical applications. *Green Processing and Synthesis*. 2022, vol. 11, no. 1, pp. 44-63.
- [13] MINO, L., NEGRI, C., SANTALUCIA, R., CERRATO, G., SPOTO, G., & MARTRA, G. Morphology, surface structure and water adsorption properties of TiO<sub>2</sub> nanoparticles: A comparison of different commercial samples. *Molecules*. 2020, vol. 25, no. 20, 4605.
- [14] ALIVISATOS, A. P. Perspectives on the physical chemistry of semiconductor nanocrystals. *The Journal of Physical Chemistry*. 1996, vol. 100, no. 31, pp. 13226-13239.
- [15] WU, L., FU, C., & HUANG, W. Surface chemistry of TiO<sub>2</sub> connecting thermal catalysis and photocatalysis. *Physical Chemistry Chemical Physics*. 2020, vol. 22, no. 18, pp. 9875-9909.
- [16] SONG, M., LU, Z., & LI, D. Phase transformations among TiO<sub>2</sub> polymorphs. *Nanoscale*. 2020, vol. 12, no. 45, pp. 23183-23190.
- [17] MOHAMAD, M., HAQ, B. U., AHMED, R., SHAARI, A., ALI, N., & HUSSAIN, R. A density functional study of structural, electronic and optical properties of titanium dioxide: Characterization of rutile, anatase and brookite polymorphs. *Materials Science in Semiconductor Processing*. 2015, vol. 31, pp. 405-414.
- [18] MAHDJOUB, N., ALLEN, N., KELLY, P., & VISHNYAKOV, V. Thermally induced phase and photocatalytic activity evolution of polymorphous titania. *Journal of Photochemistry and Photobiology A: Chemistry*. 2010, vol. 210, no. 2-3, pp. 125-129.
- [19] LANCE, R. A. Optical analysis of titania: band gaps of brookite, rutile and anatase. 2018.
- [20] BONKERUD, J., ZIMMERMANN, C., WEISER, P. M., VINES, L., & MONAKHOV, E. V. On the permittivity of titanium dioxide. *Scientific reports*. 2021, vol. 11, no. 1, 12443.
- [21] CHEN, X. D., WANG, Z., LIAO, Z. F., MAI, Y. L., & ZHANG, M. Q. Roles of anatase and rutile TiO<sub>2</sub> nanoparticles in photooxidation of polyurethane. *Polymer testing*. 2007, vol. 26, no. 2, pp. 202-208.
- [22] HANAOR, D. A., & SORRELL, C. C. Review of the anatase to rutile phase transformation. *Journal of Materials Science*. 2011, vol. 46, pp. 855-874.

- [23] ZHANG, H., & BANFIELD, J. F. Understanding polymorphic phase transformation behavior during growth of nanocrystalline aggregates: insights from TiO<sub>2</sub>. *The Journal of Physical Chemistry B*. 2000, vol. 104, no. 15, pp. 3481-3487.
- [24] WANG, H. E., CHEN, Z., LEUNG, Y. H., LUAN, C., LIU, C., TANG, Y., ... & LEE, S. T. Hydrothermal synthesis of ordered single-crystalline rutile TiO<sub>2</sub> nanorod arrays on different substrates. *Applied Physics Letters*. 2010, vol. 96, no. 26.
- [25] ANWAR, M. S., KUMAR, S., AHMED, F., ARSHI, N., LEE, C. G., & KOO, B. H. One step synthesis of rutile TiO<sub>2</sub> nanoparticles at low temperature. *Journal of Nanoscience and Nanotechnology*. 2012, vol. 12, no. 2, pp. 1555-1558.
- [26] BORSE, P. H., KANKATE, L. S., DASSENOY, F., VOGEL, W., URBAN, J., & KULKARNI, S. K. Synthesis and investigations of rutile phase nanoparticles of TiO<sub>2</sub>. *Journal of Materials Science: Materials in Electronics*. 2002, vol. 13, pp. 553-559.
- [27] PARK, N. G., CHANG, S. H., Van de LAGEMAAT, J., KIM, K. J., & FRANK, A. J. Effect of Cations on the Open-Circuit Photovoltage and the Charge-Injection Efficiency of Dye-Sensitized Nanocrystalline Rutile TiO<sub>2</sub> Films. *Bulletin-Korean Chemical Society*. 2000, vol. 21, no. 10, pp. 985-988.
- [28] DALLINGER, D., LEHMANN, H., MOSELEY, J. D., STADLER, A., & KAPPE, C. O. Scale-up of microwave-assisted reactions in a multimode bench-top reactor. *Organic Process Research & Development*. 2011, vol. 15, no. 4, pp. 841-854.
- [29] ULLATTIL, S. G., & PERIYAT, P. (2015). Green microwave switching from oxygen rich yellow anatase to oxygen vacancy rich black anatase TiO<sub>2</sub> solar photocatalyst using Mn (II) as 'anatase phase purifier'. *Nanoscale*. 2015, vol. 7, no. 45, pp. 19184-19192.
- [30] ZHANG, H., CHEN, B., BANFIELD, J. F., & WAYCHUNAS, G. A. Atomic structure of nanometer-sized amorphous TiO<sub>2</sub>. *Physical Review B—Condensed Matter and Materials Physics*. 2008, vol. 78, no. 21, 214106.
- [31] NAGARAJ, G., MOHAMMED, M. K., ABDULZAHRAA, H. G., SASIKUMAR, P., KARTHIKEYAN, S., & TAMILARASU, S. Effects of the surface of solar-light photocatalytic activity of Ag-doped TiO<sub>2</sub> nanohybrid material prepared with a novel approach. *Applied Physics A*. 2021, vol. 127, no. 4, 269.
- [32] MATOSSI, F. The vibration spectrum of rutile. *The Journal of Chemical Physics*. 1951, vol. 19, no. 12, pp. 1543-1546.
- [33] ZANATTA, A. R. A fast-reliable methodology to estimate the concentration of rutile or anatase phases of TiO<sub>2</sub>. *AIP advances*. 2017, vol. 7, no. 7.
- [34] BOROWICZ, P., LATEK, M., RZODKIEWICZ, W., ŁASZCZ, A., CZERWINSKI, A., & RATAJCZAK, J. Deep-ultraviolet Raman investigation of silicon oxide: thin film on silicon substrate versus bulk material. *Advances in Natural Sciences: Nanoscience and Nanotechnology*. 2012, vol. 3, no. 4, 045003.
- [35] SAHU, D. P., & JAMMALAMADAKA, S. N. Detection of bovine serum albumin using hybrid TiO<sub>2</sub> + graphene oxide based Bio-resistive random access memory device. *Scientific reports*. 2019, vol. 9, no. 1, 16141.
- [36] KUANG, J., XING, Z., YIN, J., LI, Z., TAN, S., LI, M., ... & ZHOU, W. Ti<sup>3+</sup> self-doped rutile/anatase/TiO<sub>2</sub> (B) mixed-crystal tri-phase heterojunctions as effective visible-light-driven photocatalysts. *Arabian Journal of Chemistry*. 2020, vol. 13, no. 1, pp. 2568-2578.